

Detecting climate signals cascading through levels of biological organization

Received: 5 December 2022

Accepted: 10 July 2023

Published online: 14 August 2023



Marlène Gamelon^{1,2}✉, Stéphanie Jenouvrier³, Melanie Lindner^{4,5},
Bernt-Erik Sæther² & Marcel E. Visser^{4,5}

Threats to species under climate change can be understood as a time at which the signal of climate change in ecological processes emerges from the noise of ecosystem variability, defined as ‘time of emergence’ (ToE). Here we show that ToE for the great tit (*Parus major*) will occur earlier at the level of population size than trait (laying date) and vital rates (survival, recruitment) under the RCP 8.5 scenario, suggesting an amplified climate change signal at the population level. ToE thus varies across levels of biological organization that filter trends and variability in climate differently. This has implications for the detection of climate impacts on wild species, as a shift in population size may precede changes in traits and vital rates. Further work would need to identify the ecological level that may experience an earlier detection of the climate signal for species with contrasting life histories, climate trends and variability.

The impact of anthropogenic climate change on wildlife populations is a topic of profound concern. Climate change occurs in the context of broadband natural climate variability, often making it difficult to discern the explicit effects of long-term change driven by forced response to GHG. In addition, ecological responses to environmental variation are stochastic with multiple sources of variation, including observed and unobserved variability in abiotic and biotic factors that interact with natural climate variability. Accordingly, detecting responses to anthropogenically forced changes in climate is challenging¹. This is, however, crucial for the detection and attribution of ecological responses to climate change because changes in climate have direct impacts on ecosystem processes and society².

To detect changes in climate, climatologists have extensively used the concept of time of emergence in climate (ToE_{climate})^{3,4}. This defines the point in time when the signal of climate change emerges from the noise of natural climate variability. It has been applied, for instance, on changes in temperature³, rainfall⁵ and polar climate^{1,4}. Here we apply this concept for the first time across levels of ecological organization to identify the time at which the signal of climate change in ecological processes emerges from the stochastic noise associated with natural

climate and ecological variability (time of emergence, ToE). We assess the ToE from trait (ToE_{trait}) to vital rates (for example, survival or recruitment; ToE_{vital}) and population size (ToE_{pop}) (Fig. 1) to study how the climate signal cascades through the levels of biological organization. Climate-induced changes in resources that influence fitness-related traits are expected to generate changes in vital rates, which lead to population-level responses. We may thus expect that the ToE is delayed across levels of biological organization, occurring earlier for traits than for vital rates and population size^{6–8}. However, those responses depend on the sensitivity of vital rates to climate variation and the sensitivity of population growth rate to changes in vital rates, potentially driving more complex patterns across levels of biological organization^{1,8,9}.

There are not many systems for which this hypothesis can be tested because it requires long-term data at various levels of biological organization. Here we use one of the best long-term ecological time series study systems on the great tit (*Parus major*) from the Hoge Veluwe National Park in the Netherlands between 1985 and 2020 (Fig. 1). The great tit is a short-lived small passerine bird species abundant in European gardens and woodlands, and it is not migratory. Global warming influences this population in several ways. In spring,

¹Laboratoire de Biométrie et Biologie Evolutive, UMR 5558 CNRS, Université Claude Bernard Lyon 1, Villeurbanne, France. ²Department of Biology, Centre for Biodiversity Dynamics, Norwegian University of Science and Technology, Trondheim, Norway. ³Biology Department, Woods Hole Oceanographic Institution, Woods Hole, MA, USA. ⁴Department of Animal Ecology, Netherlands Institute of Ecology (NIOO-KNAW), Wageningen, the Netherlands.

⁵Chronobiology Unit, Groningen Institute for Evolutionary Life Sciences (GELIFES), University of Groningen, Groningen, the Netherlands.

✉e-mail: marlene.gamelon@cnrs.fr

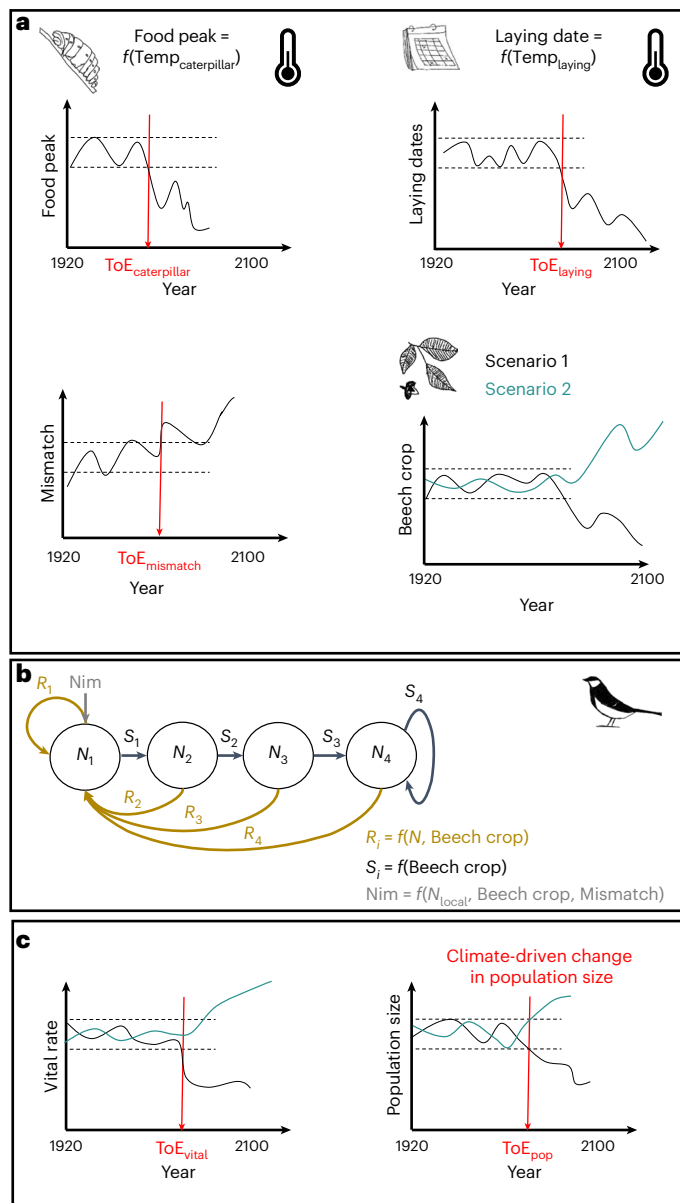


Fig. 1 | Schematic illustration of the general approach. a, Forecasted caterpillar peak dates and great tit laying dates as function (f) of temperatures (Temp), mismatch between caterpillar peak date and laying date, and beech crop production (two scenarios) in the studied great tit population expected from 1920 to 2100. From the ecological time series, the points in time when climate-driven signals in food peak, laying and mismatch can be distinguished from noise (ToE) are identified. **b**, Great tit life cycle showing age-specific vital rates (survival S_i , recruitment R_i) and the number of immigrants joining the population (Nim) as functions of mismatch, beech crop and density N . **c**, Forecasted vital rates and great tit population size from 1920 to 2100 according to expected mismatch under global warming and beech crop (two scenarios). From the time series of vital rates and population sizes, the points in time when climate-driven signals in vital rates ($\text{ToE}_{\text{vital}}$) and population size (ToE_{pop}) can be distinguished from noise are identified.

warmer temperatures lead to an advanced peak date of caterpillar biomass, an important food resource for great tits for feeding their offspring during the breeding season. However, the advancement in laying dates is slower than the advancement in food peak date, leading to a phenological mismatch between offspring requirements and food peak¹⁰. This mismatch influences the vital rates of great tits¹¹. In summer, warmer temperatures are expected to influence the intensity and

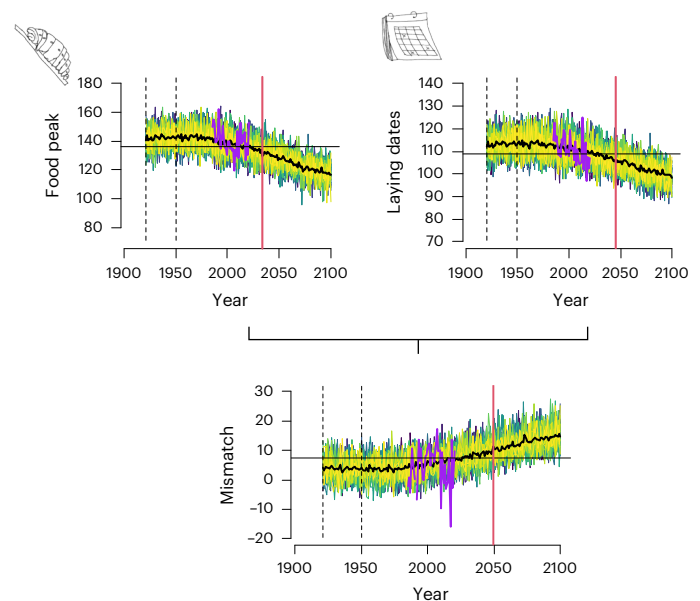


Fig. 2 | Caterpillar peak dates, great tit laying dates and their mismatch forecasted under global warming in the studied great tit population between 1920 and 2100. Each line corresponds to one climate scenario (40 in total); the black line corresponds to the mean. Vertical dotted lines indicate the historical period (1922–1950), the horizontal line indicates the lower bound of the 66% interval during that period and the vertical red line corresponds to the ToE. Annual observed values between 1985 and 2020 are shown in thick purple.

frequency of beechnut production (*Fagus sylvatica*)^{12,13}, an important food resource for great tits in winter, also affecting their vital rates¹⁴. Taking advantage of this unique system to quantify the ToE across biological levels of organization, we identified the point in time when climate-driven signals in trait (laying date), vital rates (survival, recruitment) and population dynamics can be distinguished from noise by constructing prediction intervals of ecological projections using the Community Earth System Model Large Ensemble (CESM-LE)¹⁵.

We first quantified the ToE in caterpillar peak dynamics ($\text{ToE}_{\text{caterpillar}}$). Using the established relationship between spring temperatures and caterpillar peak (period 1985–2020)¹⁶, we projected caterpillar peak dynamics under a high emission climate scenario with no policy intervention (representative concentration pathway (RCP) 8.5 scenario) back in the past and into the future, from 1920 to 2100. The peak date of caterpillar biomass advanced over time¹⁶, with an expected $\text{ToE}_{\text{caterpillar}}$ in 2034, if we only account for natural climate variability (Fig. 2). When many sources of ecological stochasticity were included in the projections, such as uncertainty in parameter estimates and process variance corresponding to unexplained temporal environmental stochasticity beyond that explained by climate, $\text{ToE}_{\text{caterpillar}}$ was detected later, in 2049 (Extended Data Fig. 1).

Second, we quantified the ToE in trait dynamics, namely laying date ($\text{ToE}_{\text{laying}}$). Using the established relationship between spring temperatures and laying dates (period for example)¹⁶, we projected laying dates dynamics from 1920 to 2100. Laying occurred earlier and earlier over years, with an expected $\text{ToE}_{\text{laying}}$ in 2045 and 2068 (with natural climate variability only and with all sources of uncertainties, respectively) (Fig. 2 and Extended Data Fig. 1). Under warmer spring conditions, directional selection for earlier laying has been reported in a plethora of species^{11,17–23}. The shift in laying date has been interpreted as a phenotypic plastic response to increasing temperatures, tracking the advance in the phenology of the food peak^{24–27}. Our results demonstrate that the difference between laying dates and date of the food peak, the so-called phenological mismatch (Fig. 1), might not be detectable before 2100 when including many sources of ecological

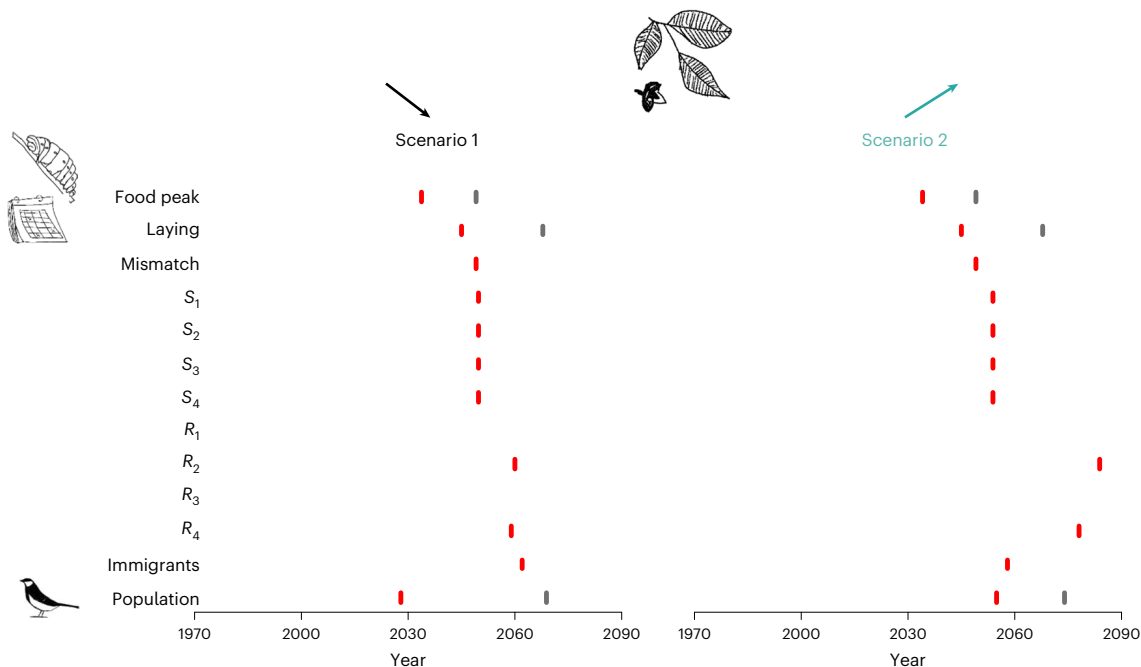


Fig. 3 | ToE from caterpillar peak dates to population size in the Hoge Veluwe great tit population. Columns show the ToE for the two scenarios of beech crop production (scenario 1, decreasing production by 2100; scenario 2, increasing

production) for the different levels of biological organization (in rows). ToE when only climate uncertainty is accounted for is shown in red and ToE when all sources of ecological uncertainties are accounted for is in grey.

uncertainties in the projections (Extended Data Fig. 1). However, when only natural climate variability was accounted for in the modelling, the time of emergence for mismatch ($\text{ToE}_{\text{mismatch}}$) was detectable and expected to occur in 2049 (Fig. 2). Increasing ecological complexity delays the $\text{ToE}_{\text{mismatch}}$ as we expected, but mainly through the interaction with environmental stochasticity.

Third, thanks to the individual long-term monitoring of great tits, we estimated annual age-specific great tit vital rates (survival, recruitment) using a state-of-the-art integrated population model^{28–31} (period 1985–2020, Extended Data Fig. 2). Annual vital rates were linked to past beechnut production, mismatch and density (period 1985–2020, Supplementary Table 1). Then we projected age-specific vital rates by 2100 under expected future conditions of mismatch and beechnut production and quantified the $\text{ToE}_{\text{vital}}$. Beechnut production is expected to change in the future^{32–34}, but there is currently no predictive model available for this food resource. Therefore, we simulated two extreme scenarios, one of decreasing beechnut production by 2100 and another of increasing production (Extended Data Fig. 3). Under the scenario of decreasing beechnut production (scenario 1), we found a decrease in vital rates over time, with a $\text{ToE}_{\text{vital}}$ between 2050 and 2060 for most of the ages when we accounted only for natural climate variation (Fig. 3 and Extended Data Fig. 4). When all sources of ecological uncertainties were accounted for, $\text{ToE}_{\text{vital}}$ was not detectable before 2100 (Fig. 3 and Extended Data Fig. 5). Similarly, under the scenario of increasing beechnut production (scenario 2), we found an increase in vital rates over time, with a $\text{ToE}_{\text{vital}}$ between 2054 and 2084 for most of them when we accounted for natural climate variability only (Fig. 3 and Extended Data Fig. 6). Interestingly, the $\text{ToE}_{\text{vital}}$ occurred earlier for survival than recruitment rates because of a stronger signal on survival. While the $\text{ToE}_{\text{vital}}$ did not differ much between the two scenarios for survival, it is delayed by up to 20 years for recruitment under the scenario of increasing, compared to decreasing, beechnut production. The climate-driven signals in recruitment rates by beechnut production were obscured by density dependence, which plays a stronger role under favourable conditions (that is, when there are more years with a high beech crop)

and a weaker one under poor conditions. As expected, when all sources of ecological uncertainties were accounted for, $\text{ToE}_{\text{vital}}$ was undetectable (Fig. 3 and Extended Data Fig. 7).

Finally, to quantify the ToE_{pop} , we projected the great tit population size from 1920 to 2100 by parametrizing a stochastic age-structured population model with the projected vital rates (Extended Data Figs. 4–7). Under the scenario of decreasing beechnut production, population size decreased with a ToE_{pop} in 2028 when we accounted for natural climate variability only, whereas population size increased under the scenario of increasing beechnut production with a ToE_{pop} in 2055 (Fig. 3). When all sources of ecological uncertainties were accounted for, ToE_{pop} occurred later, in 2069 under the first scenario and in 2074 under the second scenario (Fig. 3).

Remarkably, for any scenario of beech crop production, the ToE_{pop} occurred earlier than the $\text{ToE}_{\text{vital}}$ when all sources of uncertainties were accounted for. This is consistent with previous work based on numerical simulations that has shown that, under a fast rate of environmental change and low predictability, a population can decline before any apparent change in mean value of the trait⁸. Similarly, in an experimental design, a fast change in prey availability resulted in the decline of a protozoan ciliate population preceding a shift in mean body size⁸. Therefore, the ToE_{pop} can occur earlier than $\text{ToE}_{\text{vital}}$ and the detection of ToE depends on the level of biological organization considered, its sensitivity to climate (that is, magnitude and shape of the functional relationship between climate and ecological variable) and also on the amount of variability both in the climate and ecological systems.

Climate trends and variability are differently filtered by the vital rates (survival, reproduction) and the ages¹. In addition, density dependence may prolong the ToE_{pop} ¹ as illustrated here with our two scenarios of changes in beech crop production. Under the scenario of decreasing beech crop production (scenario 1), both survival and recruitment rates decrease, the magnitude of this decrease being age specific. Competition also decreases, allowing for more immigrants. The negative influence of beech crop on vital rates, only partially compensated by an increase in the number of immigrants, leads to a rapid

population decline, with an early ToE. Under the scenario of increasing beech crop production (scenario 2), survival and recruitment rates increase. However, competition also increases, leading to a weak positive effect of beech crop on recruitment rates, the latter being density-regulated³⁵. Similarly, the number of immigrants joining the population is positively influenced by beech crop, but strongly regulated by density, resulting in fewer immigrants. The positive influence of beech crop on survival rates, counterbalanced by a strong density regulation acting on the number of immigrants and on recruitment rates, leads to a moderate increase in population size, and a later ToE_{pop}.

Ecological variability is also key to detecting ToE. We found that ToE in mismatch and vital rates are not detectable before 2100 when ecological variability is accounted for, emphasizing the difficulties of detecting climate change signals in ecological processes. Thankfully, some of this noise from sampling and process errors can be reduced by increasing monitoring efforts and improving our understanding of how biological systems respond to biotic and abiotic factors.

The detection of ToE across levels of biological organization is context-specific, and the earlier detection at the population level we showed here is unlikely for semelparous species or if climate affects primarily fertility¹. In addition, several climate variables with different ToE may affect the various ecological organizational levels, hence making it difficult to predict which ecological level may experience an earlier detection of the climate signal. Future studies could build on our analysis to better understand and detect when climate-driven changes in ecosystems will clearly emerge from the ‘noise’ of variability across species with contrasting life histories inhabiting different environments (for example, diverse climate variability and trends)¹. This is particularly urgent as ecosystems have a limited ability to adapt and large changes outside past experience could be particularly devastating^{36,37}.

Online content

Any methods, additional references, Nature Portfolio reporting summaries, source data, extended data, supplementary information, acknowledgements, peer review information; details of author contributions and competing interests; and statements of data and code availability are available at <https://doi.org/10.1038/s41558-023-01760-y>.

References

- Jenouvrier, S. et al. Detecting climate signals in populations across life histories. *Glob. Change Biol.* **28**, 2236–2258 (2022).
- Malhi, Y. et al. Climate change and ecosystems: threats, opportunities and solutions. *Phil. Trans. R. Soc. B* **375**, 20190104 (2020).
- Mahlstein, I., Knutti, R., Solomon, S. & Portmann, R. W. Early onset of significant local warming in low latitude countries. *Environ. Res. Lett.* **6**, 034009 (2011).
- Landrum, L. & Holland, M. M. Extremes become routine in an emerging new Arctic. *Nat. Clim. Change* **10**, 1108–1115 (2020).
- Rojas, M., Lambert, F., Ramirez-Villegas, J. & Challinor, A. J. Emergence of robust precipitation changes across crop production areas in the 21st century. *Proc. Natl Acad. Sci. USA* **116**, 6673–6678 (2019).
- Clements, C. F., Blanchard, J. L., Nash, K. L., Hindell, M. A. & Ozgul, A. Body size shifts and early warning signals precede the historic collapse of whale stocks. *Nat. Ecol. Evol.* **1**, 0188 (2017).
- Clements, C. F. & Ozgul, A. Including trait-based early warning signals helps predict population collapse. *Nat. Commun.* **7**, 10984 (2016).
- Baruah, G., Clements, C. F., Guillaume, F. & Ozgul, A. When do shifts in trait dynamics precede population declines? *Am. Nat.* **193**, 633–644 (2019).
- Hilde, C. H. et al. The demographic buffering hypothesis: evidence and challenges. *Trends Ecol. Evol.* **35**, 523–538 (2020).
- Visser, M. E., van Noordwijk, A. J., Tinbergen, J. M. & Lessells, C. M. Warmer springs lead to mistimed reproduction in great tits (*Parus major*). *Proc. R. Soc. B* **265**, 1867–1870 (1998).
- Reed, T. E., Jenouvrier, S. & Visser, M. E. Phenological mismatch strongly affects individual fitness but not population demography in a woodland passerine. *J. Anim. Ecol.* **82**, 131–144 (2013).
- Övergård, R., Gemmel, P. & Karlsson, M. Effects of weather conditions on mast year frequency in beech (*Fagus sylvatica* L.) in Sweden. *Int. J. For. Res.* **80**, 555–565 (2007).
- Nussbaumer, A. et al. Patterns of mast fruiting of common beech, sessile and common oak, Norway spruce and Scots pine in Central and Northern Europe. *For. Ecol. Manag.* **363**, 237–251 (2016).
- Perdeck, A. C., Visser, M. E. & Van Balen, J. H. Great tit *Parus major* survival and the beech-crop cycle. *Ardea* **88**, 99–106 (2000).
- Kay, J. E. et al. The Community Earth System Model (CESM) large ensemble project: a community resource for studying climate change in the presence of internal climate variability. *Bull. Am. Meteorol. Soc.* **96**, 1333–1349 (2015).
- Visser, M. E., Lindner, M., Gienapp, P., Long, M. C. & Jenouvrier, S. Recent natural variability in global warming weakened phenological mismatch and selection on seasonal timing in great tits (*Parus major*). *Proc. R. Soc. B* **288**, 20211337 (2021).
- Both, C. & Visser, M. E. Adjustment to climate change is constrained by arrival date in a long-distance migrant bird. *Nature* **411**, 296–298 (2001).
- Porlier, M. et al. Variation in phenotypic plasticity and selection patterns in blue tit breeding time: between- and within-population comparisons. *J. Anim. Ecol.* **81**, 1041–1051 (2012).
- Gamelon, M. et al. Environmental drivers of varying selective optima in a small passerine: a multivariate, multiphasic approach. *Evolution* **72**, 2325–2342 (2018).
- Marrot, P., Charmantier, A., Blondel, J. & Garant, D. Current spring warming as a driver of selection on reproductive timing in a wild passerine. *J. Anim. Ecol.* **87**, 754–764 (2018).
- Le Vaillant, J., Potti, J., Camacho, C., Canal, D. & Martínez-Padilla, J. Fluctuating selection driven by global and local climatic conditions leads to stasis in breeding time in a migratory bird. *J. Evol. Biol.* **34**, 1541–1553 (2021).
- Vatka, E., Orell, M., Rytönen, S. & Merilä, J. Effects of ambient temperatures on evolutionary potential of reproductive timing in boreal passerines. *J. Anim. Ecol.* **90**, 367–375 (2021).
- Sæther, B.-E., Engen, S., Gustafsson, L., Grøtan, V. & Vriend, S. J. G. Density-dependent adaptive topography in a small passerine bird, the collared flycatcher. *Am. Nat.* **197**, 93–110 (2021).
- Charmantier, A. et al. Adaptive phenotypic plasticity in response to climate change in a wild bird population. *Science* **320**, 800–804 (2008).
- Matthysen, E., Adriaansen, F. & Dhondt, A. A. Multiple responses to increasing spring temperatures in the breeding cycle of blue and great tits (*Cyanistes caeruleus*, *Parus major*). *Glob. Change Biol.* **17**, 1–16 (2011).
- Charmantier, A. & Gienapp, P. Climate change and timing of avian breeding and migration: evolutionary versus plastic changes. *Evol. Appl.* **7**, 15–28 (2014).
- de Villemereuil, P. et al. Fluctuating optimum and temporally variable selection on breeding date in birds and mammals. *Proc. Natl Acad. Sci. USA* **117**, 31969–31978 (2020).
- Besbeas, P., Freeman, S. N., Morgan, B. J. T. & Catchpole, E. A. Integrating mark-recapture-recovery and census data to estimate animal abundance and demographic parameters. *Biometrics* **58**, 540–547 (2002).
- Schaub, M. & Abadi, F. Integrated population models: a novel analysis framework for deeper insights into population dynamics. *J. Ornithol.* **152**, 227–237 (2011).

30. Brooks, S. P., King, R. & Morgan, B. J. T. A Bayesian approach to combining animal abundance and demographic data. *Anim. Biodivers. Conserv.* **27**, 515–529 (2004).
 31. Schaub, M. & Kéry, M. *Integrated Population Models: Theory and Ecological Applications with R and JAGS* (Elsevier Science, 2021).
 32. Drobyshev, I., Niklasson, M., Mazerolle, M. J. & Bergeron, Y. Reconstruction of a 253-year long mast record of European beech reveals its association with large scale temperature variability and no long-term trend in mast frequencies. *Agric. For. Meteorol.* **192–193**, 9–17 (2014).
 33. Bogdziewicz, M., Kelly, D., Thomas, P. A., Lageard, J. G. A. & Hacket-Pain, A. Climate warming disrupts mast seeding and its fitness benefits in European beech. *Nat. Plants* **6**, 88–94 (2020).
 34. Bogdziewicz, M. et al. Climate warming causes mast seeding to break down by reducing sensitivity to weather cues. *Glob. Change Biol.* **27**, 1952–1961 (2021).
 35. Reed, T. E., Grøtan, V., Jenouvrier, S., Sæther, B.-E. & Visser, M. E. Population growth in a wild bird is buffered against phenological mismatch. *Science* **340**, 488–491 (2013).
 36. Beaumont, L. J. et al. Impacts of climate change on the world's most exceptional ecoregions. *Proc. Natl Acad. Sci. USA* **108**, 2306–2311 (2011).
 37. Hawkins, E. et al. Observed emergence of the climate change signal: from the familiar to the unknown. *Geophys. Res. Lett.* **47**, e2019GL086259 (2020).
- Publisher's note** Springer Nature remains neutral with regard to jurisdictional claims in published maps and institutional affiliations.
- Springer Nature or its licensor (e.g. a society or other partner) holds exclusive rights to this article under a publishing agreement with the author(s) or other rightsholder(s); author self-archiving of the accepted manuscript version of this article is solely governed by the terms of such publishing agreement and applicable law.
- © The Author(s), under exclusive licence to Springer Nature Limited 2023

Methods

General overview

To detect climate signals cascading through levels of biological organization, we constructed a reproducible three-step approach (Supplementary Fig. 1). First, long-term data should be collected from trait values, vital rates and population size. In parallel, environmental variables should be available. Different methods can be used to estimate annual vital rates and population size when the detection probability is lower than 1—for example capture–recapture models or integrated population models (IPM). When the detection probability is equal to 1, other methods such as population census or generalized linear models can be used. Second, the effects of environmental covariates on annual variation in trait values, vital rates and population size are assessed. This can be done using linear mixed models (see below). Third, these established relationships permit projecting time series of trait values, vital rates and population size under various environmental scenarios in the past and in the future to quantify the time of emergence (Supplementary Fig. 1) by linking ecological models to climate models.

Methodological approach objectives

Our methodological approach is divided into several objectives:

- (1) Forecasting food peak and estimating the point in time when climate-driven signals in caterpillar peak dates timing can be distinguished from noise ($\text{ToE}_{\text{caterpillar}}$).
- (2) Forecasting laying dates and estimating the point in time when climate-driven signals in great tit laying dates can be distinguished from noise ($\text{ToE}_{\text{laying}}$) (= $\text{ToE}_{\text{trait}}$).
- (3) Forecasting mismatch and estimating the point in time when climate-driven signals in mismatch (between laying dates and food peak) can be distinguished from noise ($\text{ToE}_{\text{mismatch}}$).
- (4) Forecasting vital rates and estimating the point in time when climate-driven signals in vital rates can be distinguished from noise ($\text{ToE}_{\text{vital}}$ for each age-specific vital rate).
- (5) Forecasting population dynamics and estimating the point in time when climate-driven signals in population can be distinguished from noise (ToE_{pop}).

To achieve objectives 1–3, we used functional relationships linking caterpillar peak dates, laying dates and mismatch to temperatures¹⁶. To achieve objectives 4–5, we built an IPM to estimate annual age-specific vital rates. We then estimated the functional relationships between environmental variables and vital rates using linear mixed models. Finally, to project the great tit population dynamics from 1920 to 2100, we simulated two beech crop production scenarios.

Study site and data collection

The studied population is located at Hoge Veluwe National Park in the Netherlands (52° 02' N, 5° 51' E), a wood of 171 ha. Great tits (*P. major*) are short-lived small passerine birds, abundant in European gardens and woodlands and, in the Netherlands, not migratory. They are cavity-nesters and readily accept nest boxes as nesting sites, making it possible to monitor the entire breeding population. They produce one or two clutches each year³⁸. In the study area, very few females breed in natural cavities and most of them breed in nest boxes³⁹. The population is open to immigration and emigration¹¹.

The data used in this study were collected between 1985 and 2020. Nest boxes were visited during the breeding season and laying dates were recorded (first egg laid). In addition, three types of demographic data were recorded. First, the total number of breeding females (C_t). As most females start to breed at one year of age, the breeding population size is a good proxy for the total number of females⁴⁰. Second, fledglings were marked with a uniquely numbered leg-ring, ringed mothers identified and unringed mothers given a ring to allow for future identifications. These unringed mothers were assumed to have immigrated into the population during the year in question. The following year, they are

then considered to be local females. Overall, 2,204 breeding females of known age (local and immigrant) were monitored, providing capture–recapture (CMR) data of known age females. We grouped the breeding birds of known age into four age classes: (1) corresponding to the first year of breeding (that is, second calendar year of life); (2) corresponding to the second year of breeding; (3) corresponding to the third year of breeding; and (4) breeding females in their fifth calendar year of life and older. Third, ringed fledglings were recorded as recruited to the breeding population if they were caught breeding in a subsequent year. From the monitoring of breeding females of known age, we reported for each year t the observed number of breeding females in age class i (B_{it}) and also the observed number of locally recruited females produced per age class i (J_{it}). In total, this type of demographic data based on reproductive success consisted of 3,675 breeding events.

Environmental data collection for food peak, mismatch, beech crop index and temperatures

Between 1985 and 2020 (except 1991), annual peak dates of caterpillar biomass (hereafter food peak) were determined⁴¹. The annual mismatch corresponded to the difference in mean laying date for great tits minus the food peak plus 33. These 33 days accounted for incubation duration and assumed that nestlings have the highest energy demand ten days after hatching¹⁶. In addition to caterpillars, beech mast is an important food resource for great tits, especially during winter when other resources are scarce. It is also indicative of seed production of other tree species^{14,39}. The beech crop index (BCI), measured as the net weight of all nuts per m², was recorded annually as a three-level index (1, 2 or 3).

Annual temperatures were recorded. Previous work showed that laying dates in this great tit population depended on spring temperatures from 11 March to 20 April (hereafter $\text{Temp}_{\text{laying}}$), whereas temperatures from 6 March to 14 May had the strongest influence on food peaks (hereafter $\text{Temp}_{\text{caterpillar}}$)¹⁶. We thus recorded mean daily temperatures during these two time windows. We standardized $\text{Temp}_{\text{laying}}$ and $\text{Temp}_{\text{caterpillar}}$ with the mean and the variance of $\text{Temp}_{\text{laying}}$ and $\text{Temp}_{\text{caterpillar}}$ observed during this period, so $\text{Temp}_{\text{laying}}$ and $\text{Temp}_{\text{caterpillar}}$ were transformed as Z scores. Temperature data were obtained from the De Bilt station of the KNMI (Royal Dutch Meteorological Institute), less than 50 km from the Hoge Veluwe field site.

Objective 1

In this population, food peak dates (in Julian date) are linked to temperatures ($\text{Temp}_{\text{caterpillar}}$) through the relationship¹⁶:

$$\text{food peak} = 138.379 (\text{s.d. } 0.629) - 7.162 (\text{s.d. } 0.629) \times \text{Temp}_{\text{caterpillar}} + 3.719 \quad (1)$$

From this relationship, we estimated past (1920–2019) and future (2020–2100) food peak dates according to the RCP 8.5 climate scenario, which considers no policy intervention. This scenario brings together 40 ensemble members diagnosing the influence of internal climate variability on projections¹⁵ and it is the preferred choice for assessing climate change impacts risks throughout the mid-century⁴². The mean and the s.d. over 1985–2020 of all members were used to transform temperatures ($\text{Temp}_{\text{caterpillar}}$) into Z scores. Thus, the mean and the s.d. used for standardizing each of the members was the mean of means and the mean of standard deviations calculated for each member. Such a rescaling allowed observed temperatures in the study site and climate scenarios (on average across all 40 of them) to be aligned between 1985 and 2020 so that they had the same mean and variance. From equation (1), we performed 100 simulations, parameters in the equation being drawn from normal distributions. This resulted in 100 simulations per member—that is, 4,000 simulations from 1920 to 2100. This gave us expected food peak dates when all sources of ecological uncertainties were accounted for, including parameter uncertainty and

process variance corresponding to unexplained temporal variation in parameters beyond that explained by climate.

After having visually controlled for a good match between observed food peak dates and predicted dates (period 1985–2020, Fig. 2), we selected a historical time window during which food peak dates were stable over time (1922–1950, slope of the regression between food peak dates and years during this time window: 0.032 (s.d. 0.025)). We computed the lower bound ($LB_{\text{caterpillar}}$) of the 66% prediction interval for food peak dates during this historical period, and determined the point in time when the upper bound ($UB_{\text{caterpillar}}$) of the 66% prediction interval for food peak dates became lower than $LB_{\text{caterpillar}}$. This point corresponded to the time of emergence for food peak ($ToE_{\text{caterpillar}}$). In addition, we forecasted food peak dates but we only accounted for climate uncertainty in the projections. To do so, we turned off standard errors and σ (the last term) in equation (1) to obtain 40 projections of food peak dates from 1920 to 2100—that is, one projection per member.

Objective 2

We replicated the same procedure for laying dates. In this population, laying dates (in Julian date) are linked to temperatures ($Temp_{\text{laying}}$) through the relationship¹⁶:

$$\text{laying date} = 110.980 (\text{s.d. } 0.582) - 4.947 (\text{s.d. } 0.590) \times Temp_{\text{laying}} + 3.493 \quad (2)$$

We estimated the expected annual laying dates between 1920 and 2100 according to the RCP 8.5 climate scenario with all sources of uncertainty and when only climate uncertainty was accounted for. We selected a historical time window during which laying dates were stable over time (1922–1950, with a slope of the regression between laying dates and years during this time window of 0.019 (s.d. 0.017)) and we identified the time of emergence for laying dates (ToE_{laying}).

Objective 3

We then calculated the mismatch between laying dates and food peak from 1920 to 2100 as the difference in expected annual laying dates minus the expected annual food peak plus 33 (ref. 16). This was done for the 4,000 simulations accounting for all sources of uncertainties and for the 40 simulations accounting for climate uncertainty only. In both cases, we identified the time of emergence for mismatch (ToE_{mismatch}).

Objectives 4 and 5

Estimating annual age-specific vital rates and densities. For populations with a recapture rate of 1, a population census can be used as a proxy of population size and survival rates can simply be estimated using a generalized linear model with binomial link function, based on whether or not the individual has been observed. Here we used an IPM to obtain accurate and precise estimates of annual population size and age-specific vital rates. Even if the recapture probability is high on the study site¹¹, still not all females may be recaptured, resulting in biased estimates of vital rates and number of individuals. There was also a possibility of double counts, for instance if one female has produced two broods but was only identified in one of them (because she has deserted one of the clutches), and a possibility that some clutches are missed (because females have bred in natural cavities). To estimate age-specific demographic rates and density while accounting for these issues, we integrated the recorded number of breeding females (C_t), CMR data of females of known age and data on reproductive success (that is, $B_{i,t}$ and $J_{i,t}$) into an IPM²⁹ (Supplementary Fig. 2). This framework allowed us to obtain the posterior median of age-specific vital rates (survival $S_{i,t}$, recruitment $R_{i,t}$), the number of local (N_{local}) and immigrant (Nim) breeding females in each age class N_i and total N (total density) for each year t with improved precision and free of observation error^{28–31,43}. The joint analysis of these three datasets thus allowed us to account for observation error associated with the recorded number of counted

breeding females⁴⁴. It also allowed us to account for the incomplete information on age structure in the monitoring data (for example, some females are of unknown age), for imperfect detection (for example, recapture probability is not 1) and for demographic stochasticity⁴⁵.

The likelihood of the IPM corresponds to the product of the likelihoods of the three different datasets, namely CMR data, reproductive success data and population counts⁴³. For CMR data of breeding females of known age, we used the Cormack–Jolly–Seber model⁴⁶, which allows estimation of annual survival between age class i and $i + 1$ ($S_{i,t}$) and annual recapture (p_t) probabilities. For data on reproductive success, the observed number of daughters locally recruited per age class i ($J_{i,t}$) is Poisson distributed with $J_{i,t} \sim \text{Poisson}(B_{i,t} \times R_{i,t})$, where R is the recruitment rate of females of age class i at year t . For the population count data, we used a state-space model⁴⁷ which consisted of a process model describing how the population size and structure changed over time as well as an observation model²⁸. We considered a pre-breeding age-structured model with the four predefined age classes.

The model was fitted within a Bayesian framework using NIMBLE (v.0.9.1)⁴⁸. We ran four independent chains with different starting values for 200,000 MCMC iterations, with a burn-in of 150,000 iterations, thinning every hundredth observation and resulting in 2,000 posterior samples. We used the Brooks and Gelman diagnostic \hat{R} to assess the convergence of the simulations and used the rule $\hat{R} < 1.1$ to determine whether convergence was reached⁴⁹. For a full description of the IPM, the priors used and the R code to fit the IPM, see Gamelon et al.⁵⁰.

Linking vital rates to BCI, mismatch and density. The IPM was used to estimate annual age-specific vital rates and densities. Once these were estimated, we linked annual age-specific vital rates and annual number of immigrants joining the local population as response variables to annual density, BCI and mismatch (from 1985 to 2020) (Fig. 1b). The same approach was adopted in the previous studies^{51–53} that first used an IPM to estimate vital rates and density, and then used regressions to link vital rates to density and/or environmental covariates. As the annual vital rates and densities are estimated in the IPM model, they are not obscured by sampling variance and observation error and thus this approach does not lead to spurious detection of density dependence^{50,54,55}. In detail, survival between two successive breeding seasons t and $t + 1$ could be affected by BCI at time t . Therefore, we linked age-specific survival rates $S_{i,t}$ (on a logit scale) to BCI at t . Because the effect of BCI on survival may be age specific, we included the interaction between age and BCI. To account for the non-independence of the survival rates among age classes of a given year, we included the year as a random effect. The linear mixed model (LMM) took the following form:

$$\text{logit}(S_{i,t}) = \mu + \beta_{1,i}a + \beta_2BCI_t + \beta_{3,i}[a \times BCI_t] + \beta_{\text{year}}\text{year} + \varepsilon_{S_{i,t}} \quad (3)$$

where μ is the intercept, a is the age class (that is, 1, 2, 3 and 4), β are the regression coefficients, year is the random effect and $\varepsilon_{S_{i,t}}$ corresponds to the residuals of the LMM. Note that the LMM was weighted by the inverse of the variance of the survival rates (on a logit scale) to account for the uncertainty associated with the survival rates estimated with the IPM.

The recruitment rate of a given breeding season t could be affected by the number of breeding females at time t in the population (density at t) and by BCI at time t . Therefore, we linked the age-specific recruitment rates $R_{i,t}$ (on a log scale) to density at t , N_t , and to BCI at t . Because the effect of BCI and density on recruitment may be age specific, we included the interaction between age and BCI and between age and density. The LMM took the following form:

$$\log(R_{i,t}) = \nu + \beta'_{1,i}a + \beta'_2BCI_t + \beta'_3N_t + \beta'_{4,i}[a \times BCI_t] + \beta'_{5,i}[a \times N_t] + \beta'_6\text{year} + \varepsilon_{R_{i,t}} \quad (4)$$

where v is the intercept, a is the age class, β' are the regression coefficients and $\varepsilon_{R_{it}}$ corresponds to the residuals of the LMM. As for survival rates, the LMM was weighted by the inverse of the variance of the recruitment rates (on a log scale) to account for the uncertainty associated with the recruitment rates estimated with the IPM.

The number of immigrants joining the population during the breeding season $t + 1$ may be influenced by BCI and mismatch as well as the number of local breeding females $N_{\text{local},t}$ at t . Therefore, we linked the number of immigrant breeding females $N_{\text{im},t+1}$ to the number of local breeding females $N_{\text{local},t}$, BCI and mismatch at t using a generalized linear model (GLM) with Poisson distribution:

$$N_{\text{im},t+1} = \eta + \beta_{1,1} \text{BCI}_t + \beta_{1,2} \text{Mismatch}_t + \beta_{1,3} N_{\text{local},t} + \varepsilon_{t+1} \quad (5)$$

where η is the intercept, β_i are the regression coefficients and ε_{t+1} corresponds to the residuals of the GLM.

Building the population model. For given conditions of BCI, mismatch and densities, age-specific survival and recruitment rates as well as the number of immigrants joining the local population may be simulated (hereafter denoted as $S_{\text{sim},t}$, $R_{\text{sim},t}$ and $N_{\text{im},t+1}$). As a result, the number of breeding females in the population $N_{\text{sim},t}$ may be simulated.

In detail, the total number of breeding females in the population at time $t + 1$, $N_{\text{sim},t+1}$, corresponded to the sum of breeding females in each age class i , $N_{\text{sim},t+1,i}$, at time $t + 1$ (Fig. 1):

$$N_{\text{sim},t+1} = N_{\text{sim},t+1,1} + N_{\text{sim},t+1,2} + N_{\text{sim},t+1,3} + N_{\text{sim},t+1,4} \quad (6)$$

- (1) As most of the immigrant breeding females were females of age class 1, we assumed that $N_{\text{sim},t+1,1}$ corresponded to the sum of the number of daughters that were locally recruited into the population $n_{\text{sim},t+1}$ (that is, produced by the breeding females of each age class) and also of the number of immigrants $N_{\text{im},t+1}$ arriving into the population:

$$N_{\text{sim},t+1,1} = n_{\text{sim},t+1} + N_{\text{im},t+1} \quad (7)$$

$n_{\text{sim},t+1}$ was modelled using a Poisson distribution to include demographic stochasticity:

$$n_{\text{sim},t+1} \sim \text{Poisson}(N_{\text{sim},t,1} \times R_{\text{sim},t,1}) + \text{Poisson}(N_{\text{sim},t,2} \times R_{\text{sim},t,2}) + \text{Poisson}(N_{\text{sim},t,3} \times R_{\text{sim},t,3}) + \text{Poisson}(N_{\text{sim},t,4} \times R_{\text{sim},t,4}) \quad (8)$$

- (2) $N_{\text{sim},t+1,2}$ corresponded to the number of females of age class 1 that survived from time t to time $t + 1$, and was modelled using a binomial process to include demographic stochasticity:

$$N_{\text{sim},t+1,2} \sim \text{Bin}(N_{\text{sim},t,1}, S_{\text{sim},t,1}) \quad (9)$$

- (3) $N_{\text{sim},t+1,3}$ and $N_{\text{sim},t+1,4}$ corresponded to the number of females in the previous age class that survived from time t to time $t + 1$:

$$N_{\text{sim},t+1,3} \sim \text{Bin}(N_{\text{sim},t,2}, S_{\text{sim},t,2}) \quad (10)$$

$$N_{\text{sim},t+1,4} \sim \text{Bin}(N_{\text{sim},t,3}, S_{\text{sim},t,3}) + \text{Bin}(N_{\text{sim},t,4}, S_{\text{sim},t,4}) \quad (11)$$

Therefore, for given conditions of BCI, mismatch and densities, $S_{\text{sim},t}$, $R_{\text{sim},t}$ and $N_{\text{im},t+1}$ may be computed. We accounted for sources of environmental stochasticity due to processes other than covariates included in the model with a covariance matrix Σ of 'random year effect' + $\varepsilon_{S_{it}}$ and 'random year effect' + $\varepsilon_{R_{it}}$. The covariance matrix was estimated and new residuals were generated from a multivariate normal distribution with covariance matrix equal to Σ . Then, $N_{\text{sim},t+1,1}$, $N_{\text{sim},t+1,2}$, $N_{\text{sim},t+1,3}$ and $N_{\text{sim},t+1,4}$, functions of $S_{\text{sim},t}$, $R_{\text{sim},t}$ and $N_{\text{im},t+1}$, may be computed and, finally, the density $N_{\text{sim},t+1}$ may be simulated.

Forecasting vital rates and population size and estimating $\text{ToE}_{\text{vital}}$ and ToE_{pop} . Using the age-structured population model described above, which accounted for the effects of BCI, mismatch and density on vital rates, we forecasted the great tit population under two simulated beech crop production scenarios.

Forecasting beech crop index under two scenarios. BCI is a categorical variable with three levels: 1 (low), 2 (medium) and 3 (high production). We simulated two extreme scenarios of beech crop production by 2100.

In the first scenario, we simulated a decrease in beech crop production in the future. The probability of having a year of low production ($P(\text{BCI} = \text{level } 1)$) increased over time, from 0.005 in 1920 to 0.9 in 2100. The probability of having a year of medium production ($P(\text{BCI} = \text{level } 2)$) was set to 0.1, the average observed between 1985 and 2020. The probability of having a year of high production ($P(\text{BCI} = \text{level } 3)$) corresponded to $1 - P(\text{BCI} = \text{level } 1) - P(\text{BCI} = \text{level } 2)$ and thus ranged from 0.895 to 0 from 1920 to 2100 (Extended Data Fig. 3, left panel). For each year, we performed 100 draws from a three-category multinomial distribution with probabilities $P(\text{BCI} = \text{level } 1)$, $P(\text{BCI} = \text{level } 2)$, $P(\text{BCI} = \text{level } 3)$. This resulted in 100 simulated time series of BCI between 1920 and 2100. These projections of BCI expressed as levels (1, 2 and 3) were used afterwards to project the great tit population size.

In the second scenario, we simulated an increase in beech crop production in the future. The probability of having a year of high production ($P(\text{BCI} = \text{level } 3)$) increased over time, from 0.005 in 1920 to 0.9 in 2100. The probability of having a year of medium production ($P(\text{BCI} = \text{level } 2)$) was set to 0.1. The probability of having a year of low production ($P(\text{BCI} = \text{level } 1)$) corresponded to $1 - P(\text{BCI} = \text{level } 2) - P(\text{BCI} = \text{level } 3)$ and thus ranged from 0.895 to 0 from 1920 to 2100 (Extended Data Fig. 3, right panel). For each year, we performed 100 draws from a three-category multinomial distribution with probabilities $P(\text{BCI} = \text{level } 1)$, $P(\text{BCI} = \text{level } 2)$, $P(\text{BCI} = \text{level } 3)$. This resulted in 100 simulated time series of BCI between 1920 and 2100.

Forecasting vital rates and great tit population size. Using trajectories of mismatch expected from 1920 to 2100 under the RCP 8.5 scenario that accounted for all sources of uncertainties (see objective 3) and simulated trajectories of BCI simulated according to the first scenario (decreasing beech crop production) as well as the age-specific densities in 1987 estimated with the IPM, we simulated 100 stochastic trajectories in vital rates and population sizes per ensemble member from 1920 to 2100, resulting in a total of 4,000 stochastic trajectories. We computed the 95% and 66% prediction intervals of the predicted age-specific vital rates, number of immigrants and total population size. We then selected a historical time window during which population size was stable over time (1922–1950, slope of the regression between population size and years during this time window: 0.092 (s.d. 0.217)) and estimated the time of emergence for population size (ToE_{pop}) and vital rates ($\text{ToE}_{\text{vital}}$). In addition, we forecasted the great tit population but accounted for climate uncertainty only in the projections. To do so, we used trajectories of mismatch expected from 1920 to 2100 that accounted for climate uncertainty only, and turned off stochasticity in equations (8)–(11) as well as the covariance matrix, to obtain 40 projections of age-specific vital rates and population sizes from 1920 to 2100—that is, one projection per member.

We replicated the exact same procedure with trajectories of BCI simulated according to the second scenario (increasing beech crop production) to obtain forecasted time series of vital rates and population size.

All these analyses were performed with R software⁵⁶.

Inclusion and ethics

The research was carried out under licence AVD801002017831 of the Centrale Commissie Dierexperimenten (CCD) in the Netherlands.

Fieldwork at the National Park de Hoge Veluwe was carried out with permission of the park.

Reporting summary

Further information on research design is available in the Nature Portfolio Reporting Summary linked to this article.

Data availability

Data used in the analysis are available at https://github.com/marleng/ToE_greattit. Data on past observed beech crop index, past observed mismatch between laying dates and food peaks, expected spring temperature according to the RCP 8.5 scenario, past observed annual age-specific population size and vital rates and their variance are provided.

Code availability

R code used for the analysis is available at https://github.com/marleng/ToE_greattit.

References

38. Husby, A., Kruuk, L. E. B. & Visser, M. E. Decline in the frequency and benefits of multiple brooding in great tits as a consequence of a changing environment. *Proc. R. Soc. B* **276**, 1845–1854 (2009).
39. Grøtan, V. et al. Spatial and temporal variation in the relative contribution of density dependence, climate variation and migration to fluctuations in the size of great tit populations. *J. Anim. Ecol.* **78**, 447–459 (2009).
40. Dhondt, A. A., Adriaensen, F., Matthysen, E. & Kempenaers, B. Nonadaptive clutch sizes in tits. *Nature* **348**, 723–725 (1990).
41. Ramakers, J. J. C., Gienapp, P. & Visser, M. E. Comparing two measures of phenological synchrony in a predator–prey interaction: simpler works better. *J. Anim. Ecol.* **89**, 745–756 (2020).
42. Schwalm, C. R., Glendon, S. & Duffy, P. B. RCP8.5 tracks cumulative CO₂ emissions. *Proc. Natl Acad. Sci. USA* **117**, 19656–19657 (2020).
43. Kéry, M. & Schaub, M. *Bayesian Population Analysis Using WinBUGS: A Hierarchical Perspective* (Academic Press, 2012).
44. Lebreton, J.-D. & Gimenez, O. Detecting and estimating density dependence in wildlife populations. *J. Wildl. Manage.* **77**, 12–23 (2013).
45. Lande, R. et al. Estimating density dependence from population time series using demographic theory and life-history data. *Am. Nat.* **159**, 321–337 (2002).
46. Lebreton, J.-D., Burnham, K. P., Clobert, J. & Anderson, D. R. Modeling survival and testing biological hypotheses using marked animals: a unified approach with case studies. *Ecol. Monogr.* **62**, 67–118 (1992).
47. de Valpine, P. & Hastings, A. Fitting population models incorporating process noise and observation error. *Ecol. Monogr.* **72**, 57–76 (2002).
48. de Valpine, P. et al. Programming with models: writing statistical algorithms for general model structures with NIMBLE. *J. Comput. Graph. Stat.* **26**, 403–413 (2017).
49. Brooks, S. P. & Gelman, A. General methods for monitoring convergence of iterative simulations. *J. Comput. Graph. Stat.* **7**, 434–455 (1998).
50. Gamelon, M. et al. Density dependence in an age-structured population of great tits: identifying the critical age classes. *Ecology* **97**, 2479–2490 (2016).
51. Hansen, B. B. et al. More frequent extreme climate events stabilize reindeer population dynamics. *Nat. Commun.* **10**, 1616 (2019).
52. Abadi, F. et al. Estimating the strength of density dependence in the presence of observation errors using integrated population models. *Ecol. Modell.* **242**, 1–9 (2012).
53. Gamelon, M. et al. Interactions between demography and environmental effects are important determinants of population dynamics. *Sci. Adv.* **3**, e1602298 (2017).
54. Freckleton, R. P., Watkinson, A. R., Green, R. E. & Sutherland, W. J. Census error and the detection of density dependence. *J. Anim. Ecol.* **75**, 837–851 (2006).
55. Schaub, M., Jakober, H. & Stauber, W. Strong contribution of immigration to local population regulation: evidence from a migratory passerine. *Ecology* **94**, 1828–1838 (2013).
56. R Development Core Team R: *A Language and Environment for Statistical Computing* (R Foundation for Statistical Computing, 2017).

Acknowledgements

We are grateful to all those who have collected data and to L. Vernooij and J. Risse for maintaining the long-term great tit database. We thank the board of the National Park of Hoge Veluwe for permission to carry out our research in their park. This work was supported by the Research Council of Norway through its Centres of Excellence funding scheme, project number 223257, by NASA grant number 80NSSC20K1289 to S.J. and by the CNRS.

Author contributions

All the authors conceived the research idea. M.G. and S.J. designed the methodology and carried out the formal analysis. M.E.V. undertook data acquisition and M.E.V. and B.-E.S. funding acquisition. M.G. wrote the original draft and created the visuals and all authors were involved with reviewing and editing the manuscript.

Competing interests

The authors declare no competing interests.

Additional information

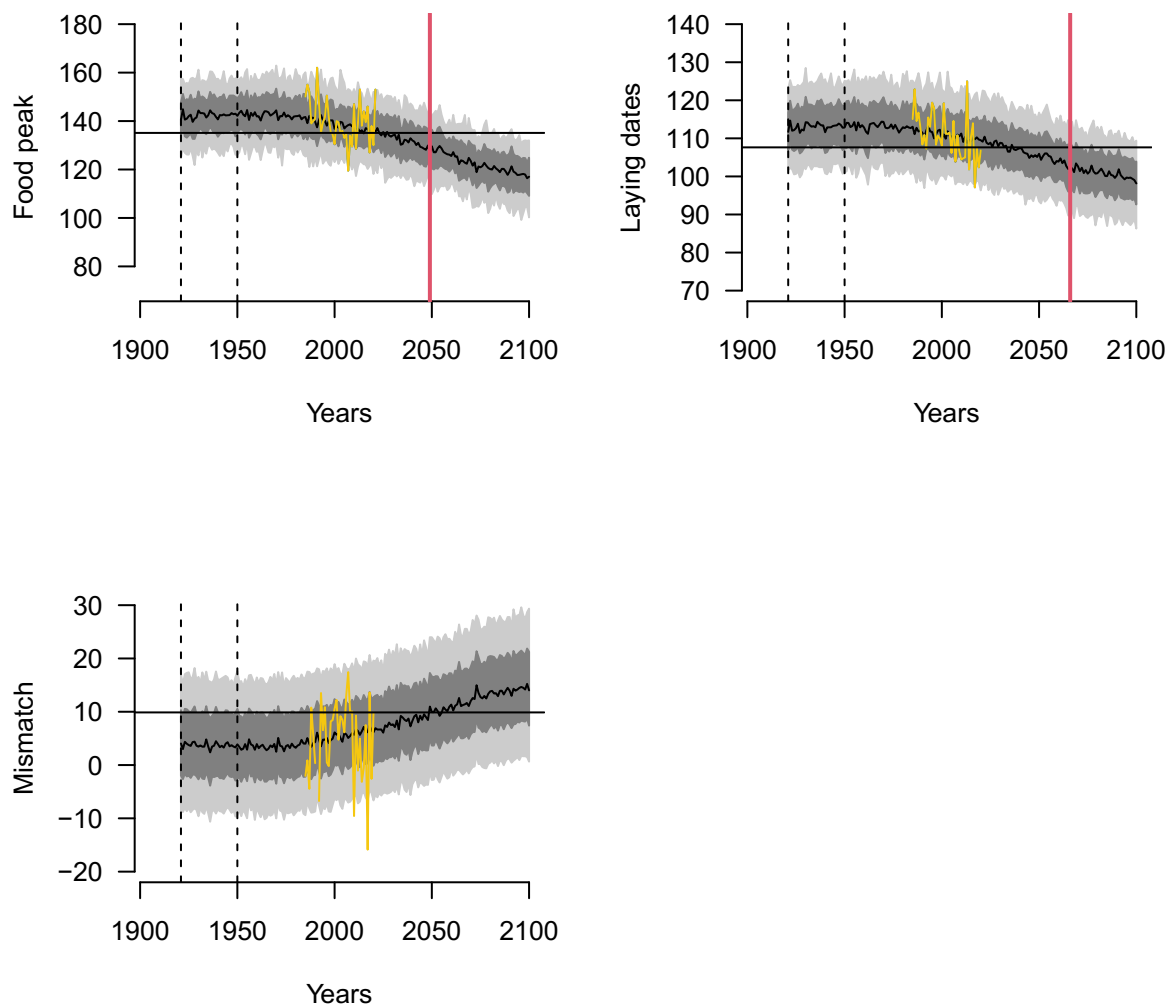
Extended data is available for this paper at <https://doi.org/10.1038/s41558-023-01760-y>.

Supplementary information The online version contains supplementary material available at <https://doi.org/10.1038/s41558-023-01760-y>.

Correspondence and requests for materials should be addressed to Marlène Gamelon.

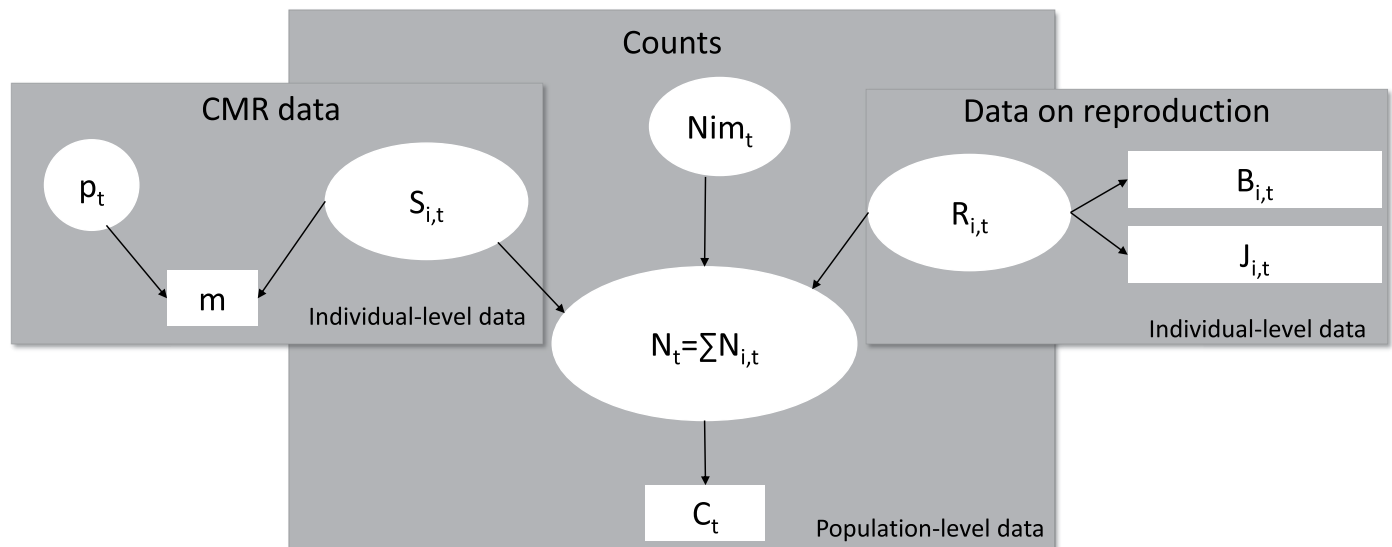
Peer review information *Nature Climate Change* thanks Qing Zhao and the other, anonymous, reviewer(s) for their contribution to the peer review of this work.

Reprints and permissions information is available at www.nature.com/reprints.



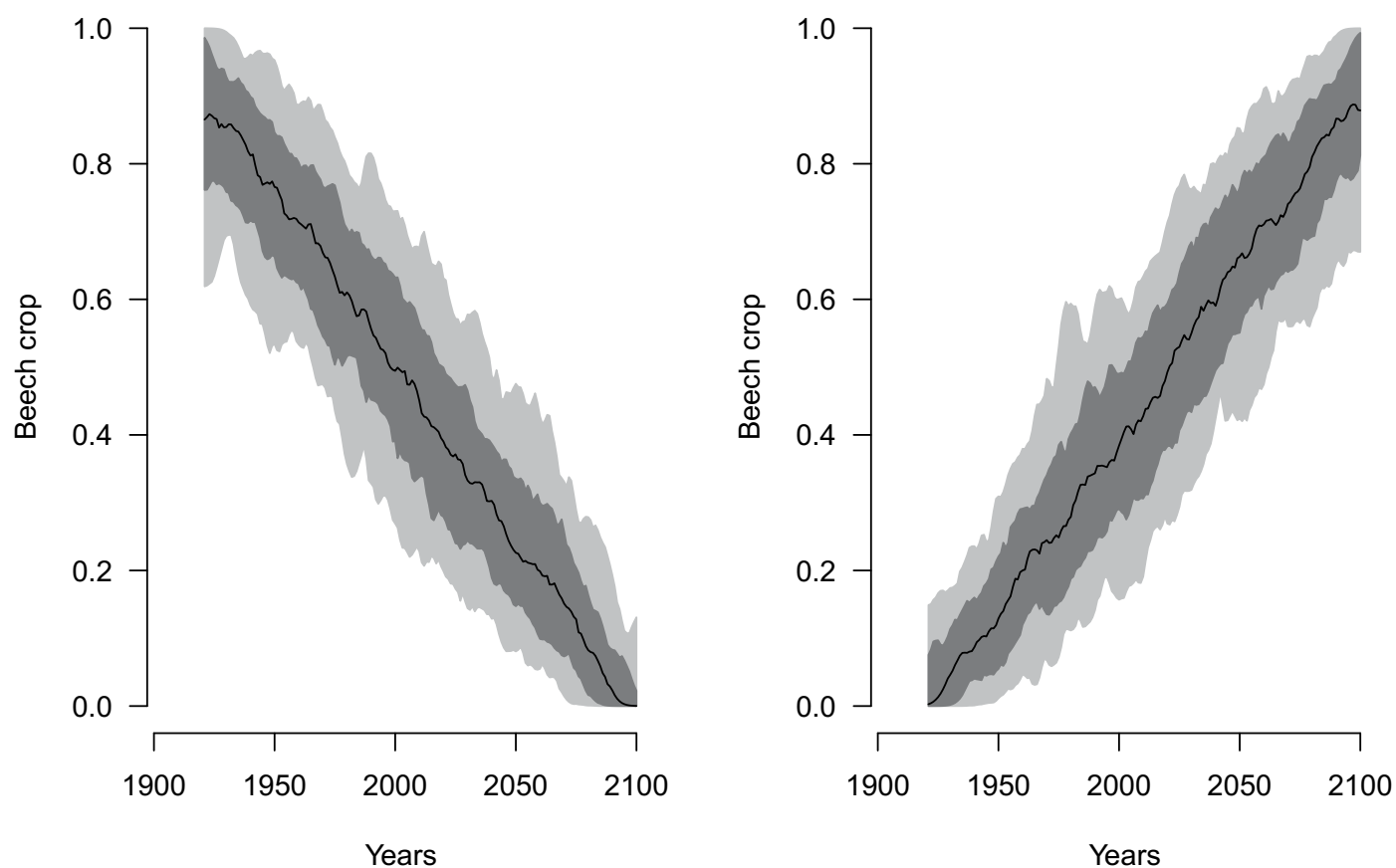
Extended Data Fig. 1 | Forecast of food peak dates, laying dates and mismatch under the RCP 8.5 scenario in the studied population between 1920 and 2100, when all sources of uncertainties are accounted for in the projections. Black line corresponds to the median, shaded dark gray corresponds to 66% and light gray to 95% prediction intervals. Vertical dotted lines indicate the historical

period (1922–1950), horizontal line indicates the lower bound of the 66% interval during that period for food peak dates and laying dates and indicates the upper bound of the interval for the mismatch. Vertical red lines correspond to the time of emergence (ToE). In yellow, annual observed values between 1985 and 2020 are provided.

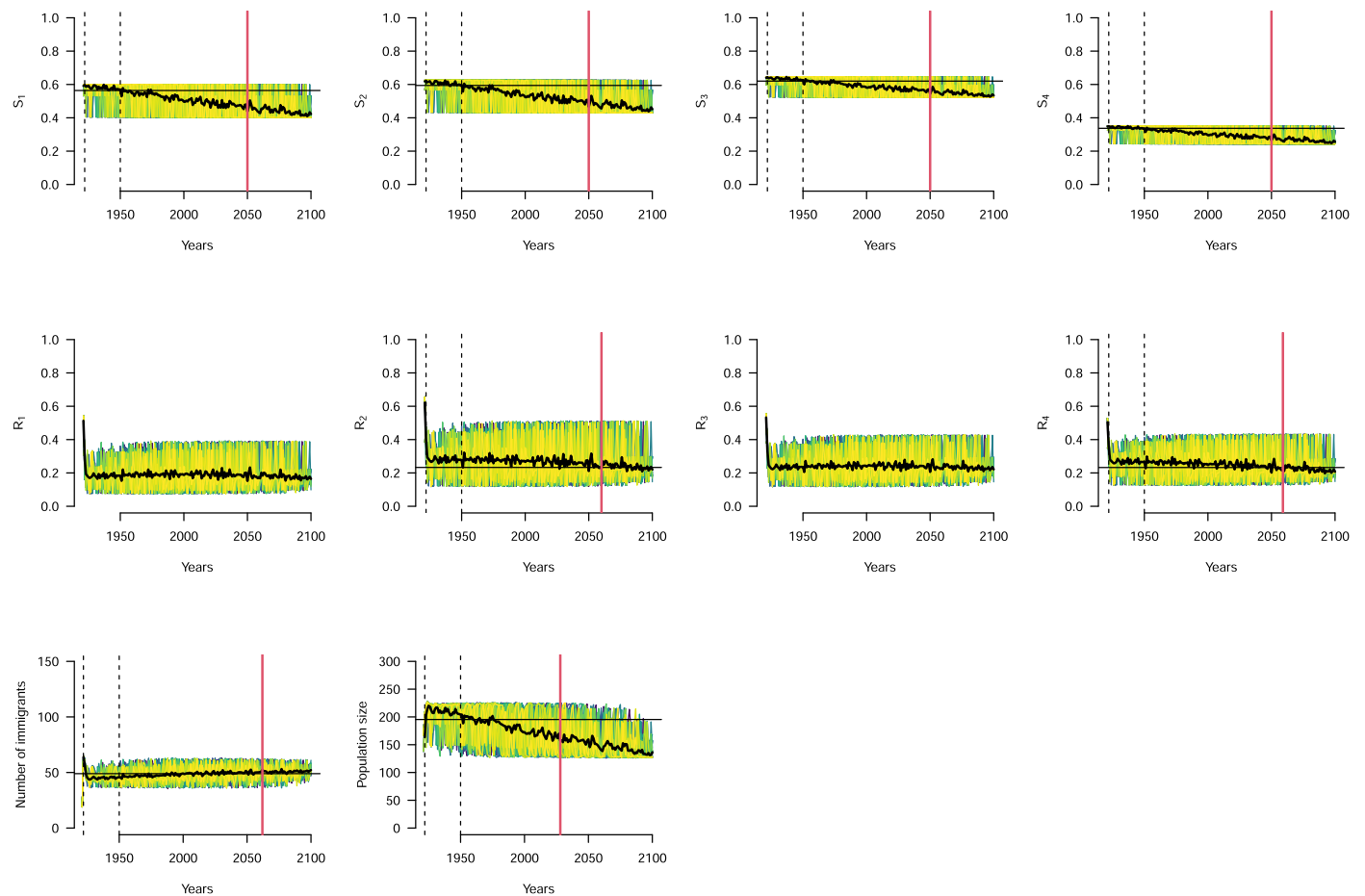


Extended Data Fig. 2 | Directed acyclic graph of the integrated population model (IPM). Squares represent the data, circles represent the parameters to be estimated. Arrows represent dependencies. Three types of demographic data are collected: CMR data (m), count data (C) and fecundity data (number of

daughters locally recruited (J) and number of mothers (B) in each age class i at year t). Parameters estimated with the IPM are the annual recapture probability p_t , annual age-specific survival $S_{i,t}$, annual age-specific recruitment $R_{i,t}$, annual number of immigrants $N_{i,t}$, and annual population size N_t .

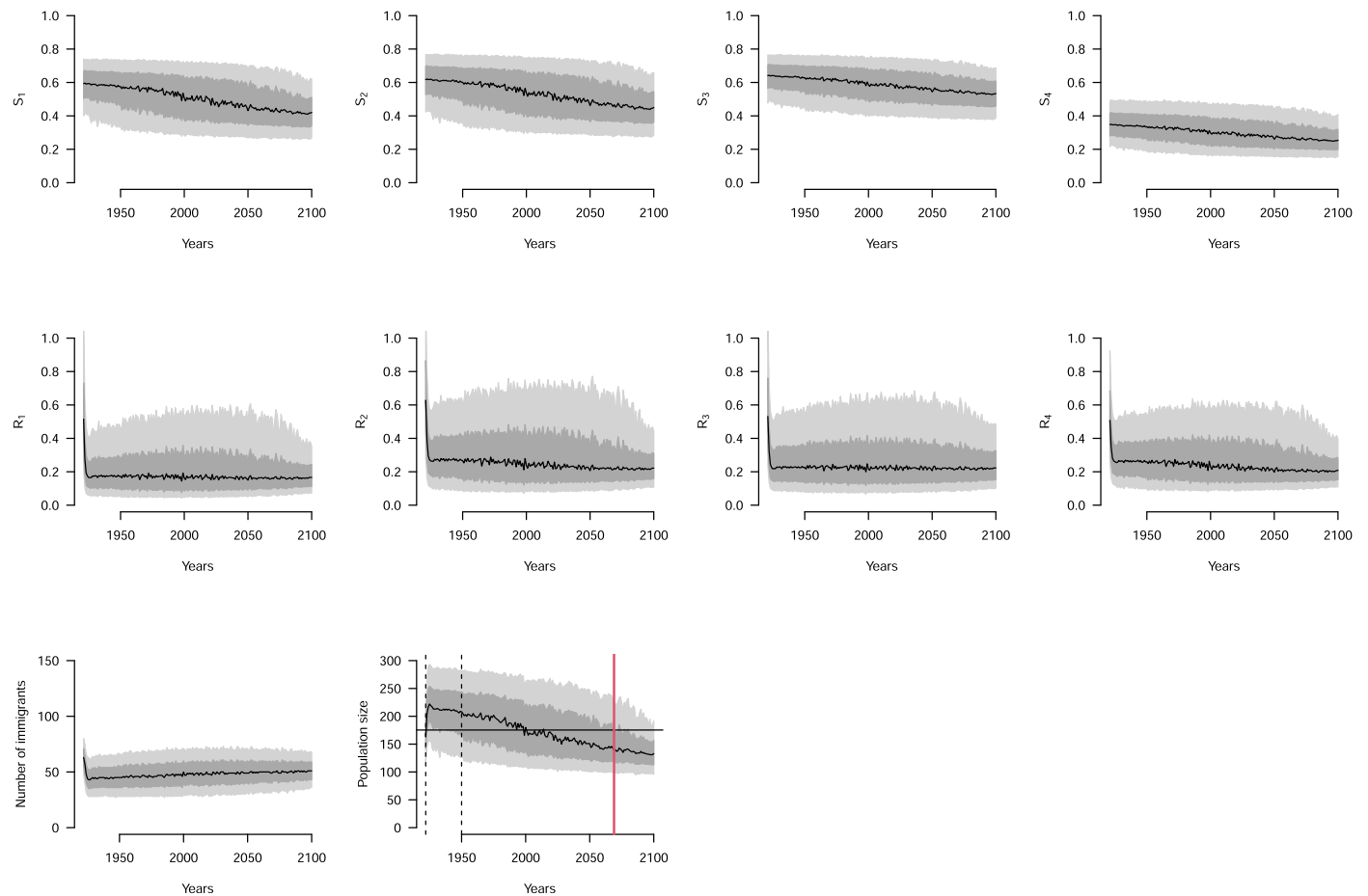


Extended Data Fig. 3 | Two extreme scenarios of beech crop production (scenarios 1 and 2). Displayed are the probabilities of having a year of high BCI (level 3)). Black lines correspond to the median, shaded dark gray corresponds to 66% and light gray to 95% prediction intervals.



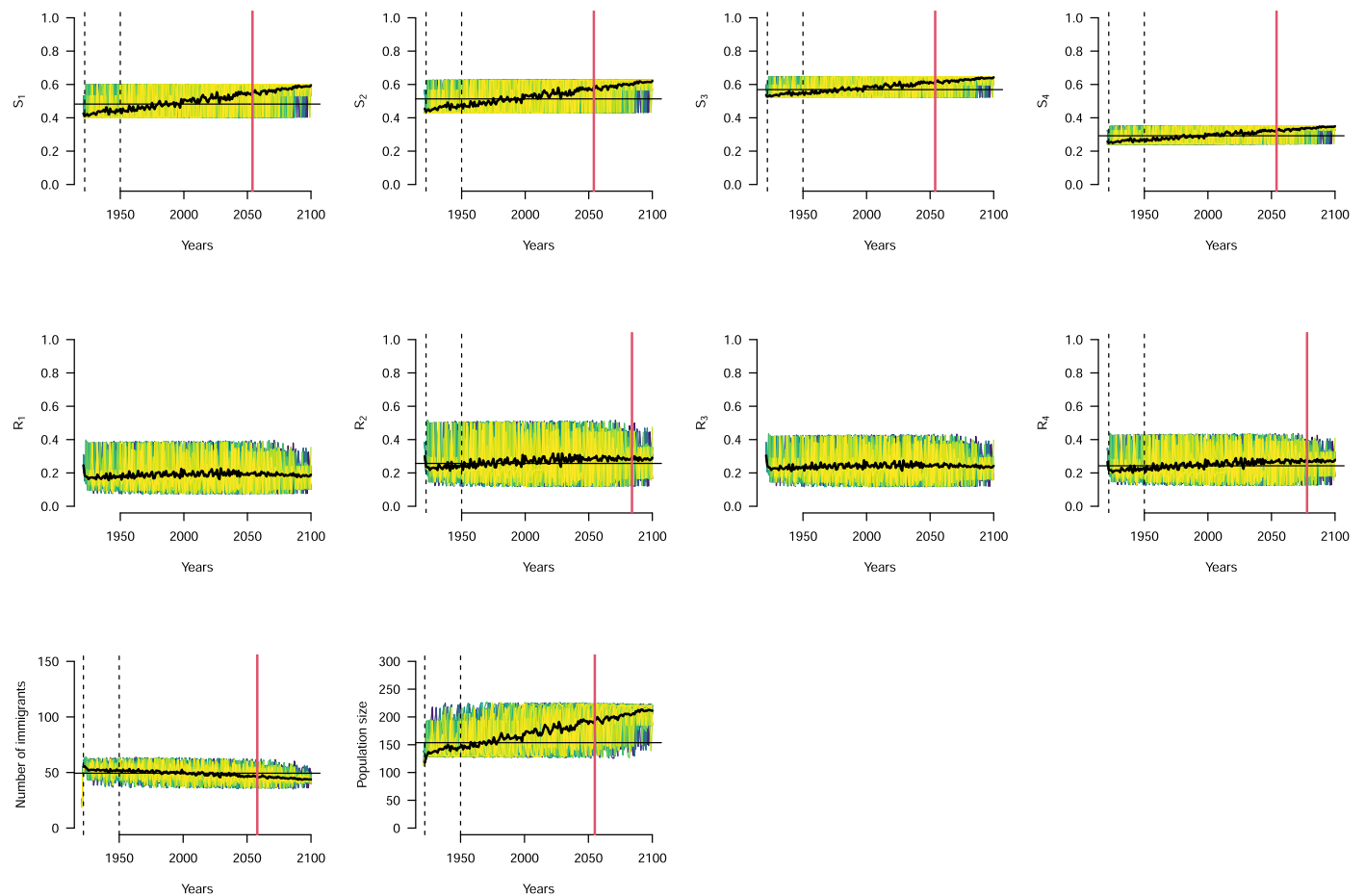
Extended Data Fig. 4 | Age-specific vital rates, number of immigrants and population size forecasted in the studied great tit population between 1920 and 2100, when climate uncertainty is accounted for in the projections, under a scenario of decreasing beech crop production (scenario 1). Each line

corresponds to one climate scenario (40 in total), and the black lines correspond to the mean. Vertical dotted lines indicate the historical period (1922–1950), horizontal lines indicate the lower bound of the 66% interval during that period. Vertical red lines correspond to the time of emergence (ToE).



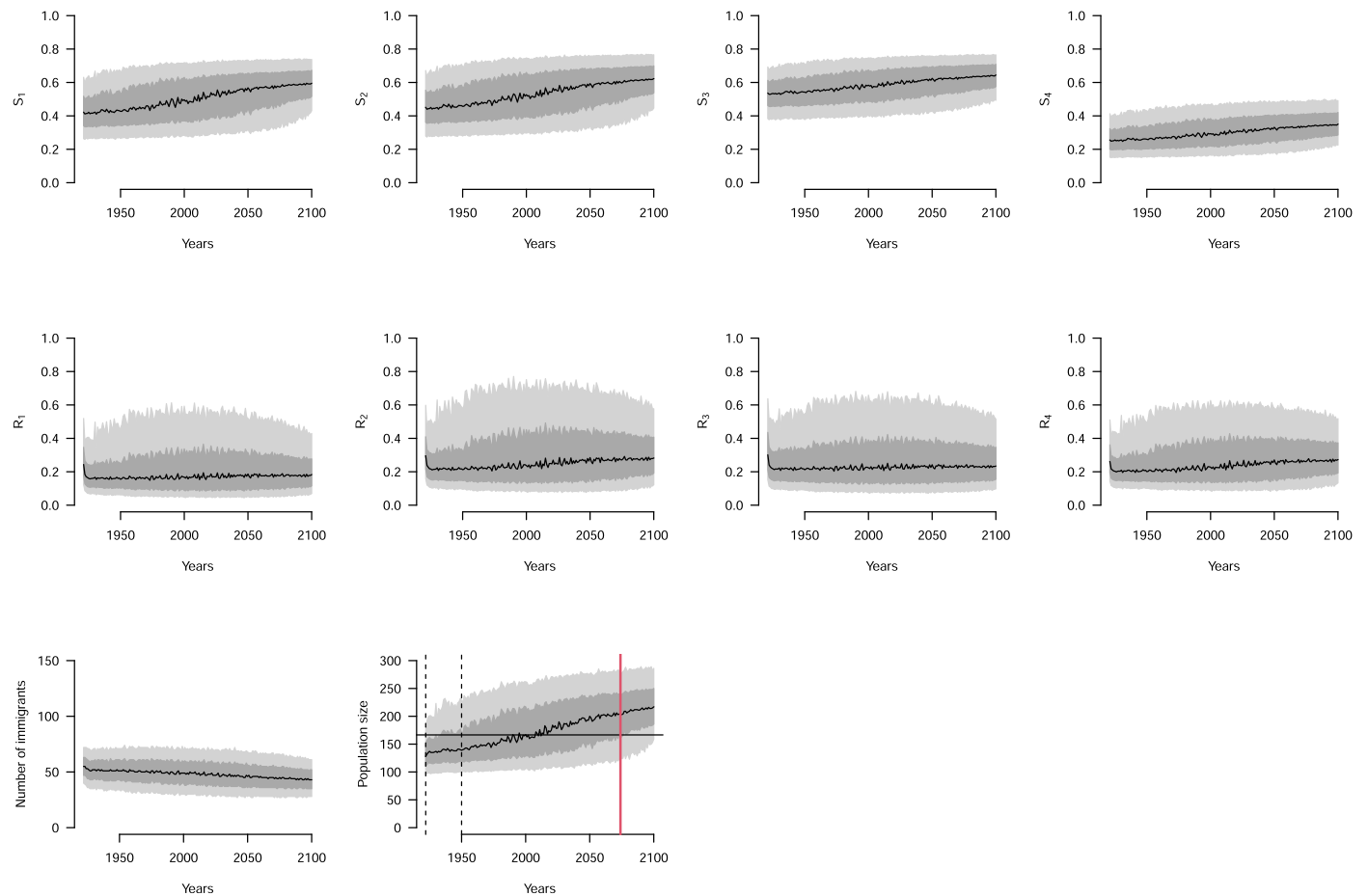
Extended Data Fig. 5 | Age-specific vital rates, number of immigrants and population size forecasted in the studied great tit population between 1920 and 2100, when all sources of ecological uncertainties are accounted for in the projections, under a scenario of decreasing beech crop production (scenario 1). Black lines correspond to the median, shaded dark gray

corresponds to 66% and light gray to 95% prediction intervals. Vertical dotted lines indicate the historical period (1922–1950), horizontal line indicates the lower bound of the 66% interval during that period. Vertical red line corresponds to the time of emergence (ToE).



Extended Data Fig. 6 | Age-specific vital rates, number of immigrants and population size forecasted in the studied great tit population between 1920 and 2100, when climate uncertainty is accounted for in the projections, under a scenario of increasing beech crop production (scenario 2). Each line

corresponds to one climate scenario (40 in total), and the black lines correspond to the mean. Vertical dotted lines indicate the historical period (1922–1950), horizontal lines indicate the upper bound of the 66% interval during that period. Vertical red lines correspond to the time of emergence (ToE).



Extended Data Fig. 7 | Age-specific vital rates, number of immigrants and population size forecasted in the studied great tit population between 1920 and 2100, when all sources of ecological uncertainties are accounted for in the projections, under a scenario of increasing beech crop production (scenario 2). Black lines correspond to the median, shaded dark gray

corresponds to 66% and light gray to 95% prediction intervals. Vertical dotted lines indicate the historical period (1922–1950), horizontal line indicates the upper bound of the 66% interval during that period. Vertical red line corresponds to the time of emergence (ToE).

Reporting Summary

Nature Portfolio wishes to improve the reproducibility of the work that we publish. This form provides structure for consistency and transparency in reporting. For further information on Nature Portfolio policies, see our [Editorial Policies](#) and the [Editorial Policy Checklist](#).

Statistics

For all statistical analyses, confirm that the following items are present in the figure legend, table legend, main text, or Methods section.

n/a Confirmed

- | | | |
|-------------------------------------|-------------------------------------|--|
| <input type="checkbox"/> | <input checked="" type="checkbox"/> | The exact sample size (n) for each experimental group/condition, given as a discrete number and unit of measurement |
| <input checked="" type="checkbox"/> | <input type="checkbox"/> | A statement on whether measurements were taken from distinct samples or whether the same sample was measured repeatedly |
| <input checked="" type="checkbox"/> | <input type="checkbox"/> | The statistical test(s) used AND whether they are one- or two-sided
<i>Only common tests should be described solely by name; describe more complex techniques in the Methods section.</i> |
| <input type="checkbox"/> | <input checked="" type="checkbox"/> | A description of all covariates tested |
| <input type="checkbox"/> | <input checked="" type="checkbox"/> | A description of any assumptions or corrections, such as tests of normality and adjustment for multiple comparisons |
| <input type="checkbox"/> | <input checked="" type="checkbox"/> | A full description of the statistical parameters including central tendency (e.g. means) or other basic estimates (e.g. regression coefficient) AND variation (e.g. standard deviation) or associated estimates of uncertainty (e.g. confidence intervals) |
| <input checked="" type="checkbox"/> | <input type="checkbox"/> | For null hypothesis testing, the test statistic (e.g. F , t , r) with confidence intervals, effect sizes, degrees of freedom and P value noted
<i>Give P values as exact values whenever suitable.</i> |
| <input type="checkbox"/> | <input checked="" type="checkbox"/> | For Bayesian analysis, information on the choice of priors and Markov chain Monte Carlo settings |
| <input checked="" type="checkbox"/> | <input type="checkbox"/> | For hierarchical and complex designs, identification of the appropriate level for tests and full reporting of outcomes |
| <input type="checkbox"/> | <input checked="" type="checkbox"/> | Estimates of effect sizes (e.g. Cohen's d , Pearson's r), indicating how they were calculated |

Our web collection on [statistics for biologists](#) contains articles on many of the points above.

Software and code

Policy information about [availability of computer code](#)

Data collection	No software was used for data collection
Data analysis	R software version 4.1.1 / NIMBLE (version 0.9.1) - Code used for the analysis is available at https://github.com/marleng/ToE_greattit (the link will be public)

For manuscripts utilizing custom algorithms or software that are central to the research but not yet described in published literature, software must be made available to editors and reviewers. We strongly encourage code deposition in a community repository (e.g. GitHub). See the Nature Portfolio [guidelines for submitting code & software](#) for further information.

Data

Policy information about [availability of data](#)

All manuscripts must include a [data availability statement](#). This statement should provide the following information, where applicable:

- Accession codes, unique identifiers, or web links for publicly available datasets
- A description of any restrictions on data availability
- For clinical datasets or third party data, please ensure that the statement adheres to our [policy](#)

Data used in the analysis are available at https://github.com/marleng/ToE_greattit (the link will be public)

Human research participants

Policy information about [studies involving human research participants and Sex and Gender in Research](#).

Reporting on sex and gender

Population characteristics

Recruitment

Ethics oversight

Note that full information on the approval of the study protocol must also be provided in the manuscript.

Field-specific reporting

Please select the one below that is the best fit for your research. If you are not sure, read the appropriate sections before making your selection.

☐ Life sciences ☐ Behavioural & social sciences ☒ Ecological, evolutionary & environmental sciences

For a reference copy of the document with all sections, see nature.com/documents/nr-reporting-summary-flat.pdf

Ecological, evolutionary & environmental sciences study design

All studies must disclose on these points even when the disclosure is negative.

Study description	Taking advantage of a unique long-term monitoring of a great tit population in the Netherlands, we determine the point in time when climate-driven signals in caterpillar peak dates timing can be distinguished from noise (ToEcaterpillar), the point in time when climate-driven signals in great tit laying dates can be distinguished from noise (ToElaying), the point in time when climate-driven signals in mismatch (between laying dates and food peak) can be distinguished from noise (ToEmism), and the point in time when climate-driven signals in vital rates and population dynamics can be distinguished from noise (ToEind and ToEpop).
Research sample	The studied population is located at Hoge Veluwe National Park in the Netherlands (52°02'N, 5°51'E), a wood of 171 ha. Great tits (<i>Parus major</i>) are cavity-nesters and readily accept nest boxes as nesting sites, making it possible to monitor the entire breeding population. The data used in this study were collected between 1985 and 2020. Nest boxes were visited during the breeding season and laying dates were recorded (1st egg laid). In addition, three types of demographic data were recorded. First, the total number of breeding females (Ct). As most females start to breed at one year of age, the breeding population size is a good proxy for the total number of females. Second, fledglings were marked with a uniquely numbered leg-ring, ringed mothers identified and unringed mothers given a ring to allow for future identifications. These unringed mothers were assumed to have immigrated into the population during the year in question. The following year, they are then considered to be local females. Third, ringed fledglings were recorded as recruited to the breeding population if they were caught breeding in a subsequent year.
Sampling strategy	Overall, 2,204 breeding females of known age (local and immigrant) were monitored, providing capture-recapture (CMR) data of known age females.
Data collection	Louis Vernooij has maintained the long-term great tit database - Marcel E. Visser has contributed to data collection and has built the research protocols.
Timing and spatial scale	The data used in this study were collected between 1985 and 2020, at Hoge Veluwe National Park in the Netherlands (52°02'N, 5° 51'E), a wood of 171 ha.
Data exclusions	No data were excluded
Reproducibility	There is no experimental findings in the present study.
Randomization	Individuals of different ages may be differently affected by density dependence and environmental covariates. We thus accounted for the age of the individuals in the analyses.
Blinding	Blinding was not relevant to our study. Data analysed come from individual long-term monitoring of wild animals.
Did the study involve field work?	<input checked="" type="checkbox"/> Yes <input type="checkbox"/> No

Field work, collection and transport

Field conditions	Annual spring temperatures were recorded (matching with the field period) between 1985 and 2020. They are discussed in the materials and methods section.
Location	The studied population is located at Hoge Veluwe National Park in the Netherlands (52°02'N, 5°51'E).
Access & import/export	The research was carried out under licence AVD801002017831 of the Centrale Commissie Dierexperimenten (CCD) in the Netherlands. Fieldwork at the National Park de Hoge Veluwe was carried out with permission of the Park.
Disturbance	<i>Describe any disturbance caused by the study and how it was minimized.</i>

Reporting for specific materials, systems and methods

We require information from authors about some types of materials, experimental systems and methods used in many studies. Here, indicate whether each material, system or method listed is relevant to your study. If you are not sure if a list item applies to your research, read the appropriate section before selecting a response.

Materials & experimental systems

n/a	Involved in the study
<input checked="" type="checkbox"/>	<input type="checkbox"/> Antibodies
<input checked="" type="checkbox"/>	<input type="checkbox"/> Eukaryotic cell lines
<input checked="" type="checkbox"/>	<input type="checkbox"/> Palaeontology and archaeology
<input type="checkbox"/>	<input checked="" type="checkbox"/> Animals and other organisms
<input checked="" type="checkbox"/>	<input type="checkbox"/> Clinical data
<input checked="" type="checkbox"/>	<input type="checkbox"/> Dual use research of concern

Methods

n/a	Involved in the study
<input checked="" type="checkbox"/>	<input type="checkbox"/> ChIP-seq
<input checked="" type="checkbox"/>	<input type="checkbox"/> Flow cytometry
<input checked="" type="checkbox"/>	<input type="checkbox"/> MRI-based neuroimaging

Animals and other research organisms

Policy information about [studies involving animals](#); [ARRIVE guidelines](#) recommended for reporting animal research, and [Sex and Gender in Research](#)

Laboratory animals	The study did not involve laboratory animals.
Wild animals	Great tits (<i>Parus major</i>) were captured each year (between 1985 and 2020) during the breeding period directly within nest boxes. They were of four different age classes: 1, corresponding to the first year of breeding (i.e., second calendar year of life); 2, corresponding to the second year of breeding; 3 corresponding to the third year of breeding; and 4, which groups breeding females in their fifth calendar year of life and older. They were released at the exact same location (within the nest) just after identification. Their fledglings were marked with a uniquely numbered leg-ring, and released in the nest boxes.
Reporting on sex	The analysis was performed on females only as we focused on females' trait (egg laying date).
Field-collected samples	The study did not involve samples collected from the field.
Ethics oversight	The research was carried out under licence AVD801002017831 of the Centrale Commissie Dierexperimenten (CCD).

Note that full information on the approval of the study protocol must also be provided in the manuscript.